Photodegradation in porous, fast-response pressure-sensitive paint under varying pressures

NATHAN S. STRASSER,[1] DAVID D. MURAKAMI,[2] E. LARA LASH,[2] JENNIFER G. COLBORN,[1] LAWRENCE A. HAND,[2] AND CHRISTOPHER S. COMBS[1,*]

[1]*Department of Mechanical, Aerospace, & Industrial Engineering, The University of Texas at San Antonio, San Antonio, TX 78249, USA*
[2]*Fluid Mechanics Laboratory, NASA Ames Research Center, Moffett Field, CA 94035, USA*
**ccombs@utsa.edu*

Abstract: Lifetime-based and ratiometric-intensity techniques are two methods for measuring surface pressure on wind tunnel models using porous, fast-response pressure-sensitive paint (fast-PSP). This paper characterizes how photodegradation under varying oxygen partial pressures impacts the intensity signal, lifetime ratio, and calibration accuracy of a platinum (II) meso-tetra(pentafluorophenyl)porphine (PtTFPP)-based fast-PSP. A temperature- and pressure-controlled test chamber was used to expose PSP coupons to excitation light at different oxygen partial pressures (P_{O2}). In the experiments, the luminescent intensity decay rate and the lifetime ratio decay rate increased by 0.1% and 0.12% per minute per kPa of P_{O2}, respectively. Calibration curves were observed to become increasingly nonlinear with higher photodegradation pressures. These trends are consistent with the effects of photodecomposition and photo-oxidation. Based on these findings, the authors propose best practices to reduce errors and improve measurement reliability, including pairing fast-PSP measurements with reference transducers for continuous calibration, reapplying and inspecting fast-PSP coatings in regions with steep pressure gradients, and defining acceptable uncertainty thresholds for a given experiment.

1. Introduction

Pressure-sensitive paint (PSP) is a tool for obtaining quantitative surface pressure measurements in wind tunnels [1-13]. Steady and unsteady pressure measurements can be made from porous, fast-response pressure-sensitive paint (fast-PSP), a variant of PSP with very high oxygen permeability, depending on the processing method used. Time-averaged processing of fast-PSP offers steady-state surface pressure measurements [14, 15]. Unsteady pressure-sensitive paint (uPSP) processing, a related approach using the same class of paint formulation, captures unsteady pressure fluctuations. Both methods rely on the luminescent properties of the paint to provide pressure data with high spatial resolution. Pressure data are typically derived from fast-PSP measurements via one of two common approaches: an intensity-based method or a luminescent lifetime method [16-18].

The intensity method involves the continuous excitation of the paint using a UV or visible LED light source to induce luminescence. Luminescence intensity decreases as local pressure increases due to oxygen quenching of the luminophore's excited states [19]. High-speed cameras are used to capture the dynamic changes in intensity. This "wind-on" intensity signal is normalized by a time-averaged "wind-off" (no-flow) intensity and compared to a laboratory calibration to determine the pressure [20]. This technique is a common method of obtaining pressure measurements with PSP and is well-documented along with many of its challenges [21-24].

A prominent and consistent observation in oxygen-sensing PSPs is the gradual decrease in luminescent intensity under prolonged excitation, a phenomenon known as photodegradation [1-3, 20, 25-39]. Over time, photodegradation of the luminescent dye leads to measurement inconsistencies [26, 31, 40]. Photodegradation is a common issue in oxygen sensors continuously exposed to light, as this exposure can generate singlet oxygen in the process [27, 28]. Photodegradation can be classified into two processes: photodecomposition and photo-oxidation. Photodecomposition occurs when a molecule dissociates into atoms, ions, and free radicals upon light exposure [41, 42]. The dissociation causes the luminescent dye to lose its ability to emit photons via fluorescence and phosphorescence. Photo-oxidation involves a molecule undergoing an oxidation reaction after exposure to light. During oxygen quenching, triplet oxygen ($^3O_2$) transitions to singlet oxygen ($^1O_2$), which is a strong oxidizing agent that can react with non-radical substances including dye molecules [20, 29, 42]. These two processes play a significant role in the photodegradation of fast-PSP, especially in wind tunnels where paint is exposed to high-intensity light and dynamic pressure conditions for extended periods. Both photodegradation and increased pressure result in decreased luminescence, making it challenging to differentiate between the two effects.

To mitigate issues associated with photodegradation in the intensity method, the lifetime-based analysis method was developed [43-45]. The lifetime method involves pulsed excitation of the paint to observe its transient luminescent response rather than directly measuring fluorescence intensity, which minimizes the sensitivity of the measurement to the excitation source intensity distribution [16, 45, 46]. In this technique, an LED lamp and camera are synchronized so that two images are recorded in rapid succession: the first image captures the rising luminescent behavior when the lamp is turned on, and the second captures the luminescent decay when the lamp is turned off [11, 16, 30]. When the lamp is off, the excited luminophore dye molecules release energy through various relaxation pathways, including radiative decay (emission of light) and non-radiative quenching by oxygen, returning the molecule to the ground state [20]. The more oxygen molecules that are present near the surface of the paint, the more likely that an excited dye molecule will be quenched by oxygen before it can radiate that excess energy as light [47, 48].

In this study, the lifetime ratio is defined as the ratio of the lamp-off to lamp-on intensity ratio rather than a direct calculation of decay time constants. The pulsed excitation method used herein approximates lifetime behavior without explicitly calculating the decay time constant [16, 17, 32, 34, 49, 50]. While the absolute intensity of the paint decreases as the luminophore photodegrades, the lamp-off to lamp-on intensity ratio has traditionally been considered constant for a given pressure, as the decay time constant should ideally not change with intensity [51]. A wind-off lifetime measurement should maintain a spatially consistent ratio before and after testing, matching the calibrated lifetime ratio at atmospheric pressure. However, previous wind tunnel tests showed that the lifetime ratio varied throughout a run and exhibited greater spatial nonuniformities than the intensity [17, 24, 45, 52].

When analyzing these data sets from previous experiments further, it was noticed that both the intensity and lifetime ratio of platinum (II) meso-tetra(pentafluorophenyl)porphine (PtTFPP)-based fast-PSP, purchased from paint supplier ISSI, do not remain consistent throughout testing and regions subjected to higher pressures during excitation change at different rates. This observation prompted us to explore the role of oxygen partial pressure (P_{O2}) in photodegradation—specifically its effects on intensity, lifetime ratio, and calibration—building on previous observations [17, 24, 52]. Previous studies have explored the decrease in PtTFPP intensity with exposure to excitation light [26, 32, 36-38]. One paper measured the overall photodegradation rate of PtTFPP at different pressures post-photodegradation, finding lower photo-bleaching at reduced ambient pressure [39]. That study examined the luminescence intensity before and after photodegradation in fast-PSP, leaving the pressure dependency of intensity during photodegradation only partially explored [39]. However, no research previously reported in the peer-reviewed literature has quantified photodegradation

effects on a PtTFPP-based fast-PSP's lifetime ratio or calibration nor investigated how pressure affects the lifetime ratio and calibration during photodegradation. While ISSI's datasheet provides an estimated 1% per minute photodegradation rate for their fast-PSP, the influence of pressure on photodegradation rates and calibration remains unclear; this work seeks to address this gap [53]. To better understand the effects of pressure on photodegradation, benchtop experiments were conducted to characterize the effect of pressure on photodegradation in this PtTFPP-based fast-PSP.

2. Photodegradation Observations in Wind Tunnel Experiments

Photodegradation effects were examined in multiple datasets collected at NASA Ames' Mach 0.6, 14" × 14" Test Cell 3 during wind tunnel experiments [2, 24, 54, 55]. Fast-PSP measurements provided data on how both the intensity and lifetime ratio changed over repeated wind tunnel tests. The fast-PSP used in the present work was formulated by Innovative Scientific Solutions, Inc. (ISSI) and used platinum (II) meso-tetra(pentafluorophenyl)porphine (PtTFPP) as the luminophore [2, 6, 24, 54, 56]. In one configuration, a block was placed on the surface coated with fast-PSP to generate pressure gradients, while in the other, measurements were obtained without the block. Wind-on data and a more detailed description of the experimental setup from these test campaigns have been previously published [2, 6, 24, 54, 57].

Fig. 1(a) provides a 3D schematic of the experimental setup with the block installed, while the top-down view in Fig. 1(b) captures the spatial percent change in intensity throughout a wind tunnel run. Here, the flow was from left to right. The upstream side of the block, where pressure was highest, showed a greater change in intensity, indicating more severe photodegradation. When photodegradation was neglected, the calculated average pressure from the second wind-off image increased to 106 kPa instead of the actual 99.7 kPa over the 5.5-second wind tunnel test. This drift accumulated over time, reducing measurement accuracy in longer test runs. Regions subjected to higher pressure exhibited larger changes from their initial intensity, confirming that pressure affected the rate of photodegradation.

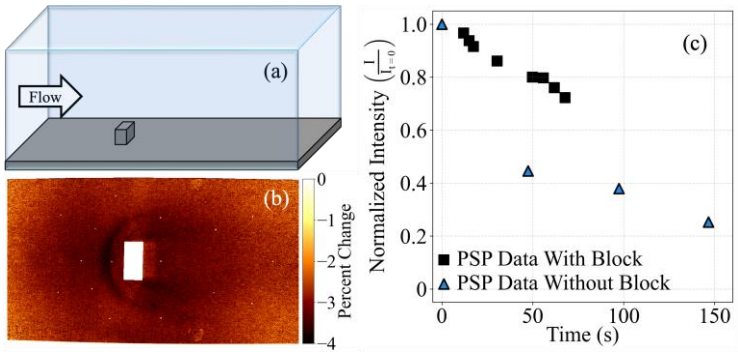

Fig. 1. (a) A 3D schematic of the experimental setup and fast-PSP surface geometry where the flow was from left to right. (b) Spatial percent change of the intensity values after 5.5 seconds of excitation light exposure. (c) Normalized fast-PSP intensity, plotted as a function of exposure time to excitation light.

Plotted in Fig. 1(c) is the normalized intensity as a function of total elapsed time, with each data point representing the average surface intensity under wind-off conditions normalized to the initial intensity of the fast-PSP surface. Overall, the data showed a consistent decrease in luminescent intensity with increased exposure time, confirming that prolonged exposure led to greater photodegradation.

Following the intensity tests, lifetime ratio measurements were performed for the block case, with prior excitation light exposure used to assess photodegradation across pressure regions. This exposure allowed for the observation of photodegradation effects on the lifetime ratios

across different pressure regions induced by the block. A threshold of -3.45% or lower was applied to the spatial intensity plot in Fig. 1(b) to define the shock region, determined by testing multiple thresholds and selecting the value that most consistently identified the area of greatest intensity change in the high-pressure region upstream of the block. The lifetime ratios from this region were then plotted as a histogram in Fig. 2(a), with the corresponding data mask shown in Fig. 2(b). This histogram was compared to that of the entire PSP-coated surface to evaluate regional differences in photodegradation. These histograms showed that the lifetime ratios within the higher-pressure region were lower than those observed across the entire PSP-coated surface, suggesting that the lifetime ratio decreased more in regions subjected to higher pressures. The observation aligned with the intensity data from Fig. 1(b), which showed greater photodegradation in higher-pressure regions.

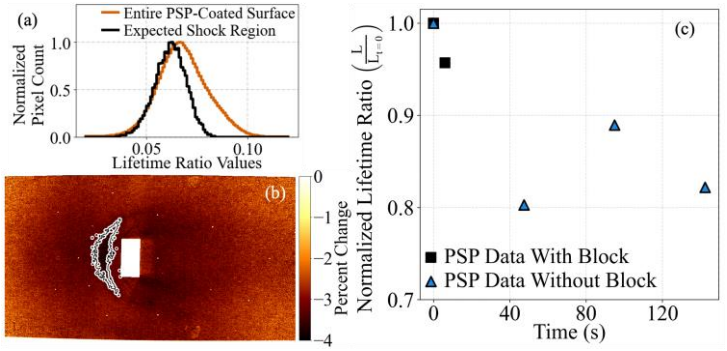

Fig. 2. (a) Histograms of lifetime ratio values for the entire lifetime ratio image and the region within the expected shock location after 42 seconds of excitation light exposure. (b) Data mask area used to isolate the shock region for lifetime ratio analysis. (c) Normalized fast-PSP lifetime ratio for experimental runs, plotted as a function of exposure time to excitation light.

Fig. 2(c) shows the cumulative change in the fast-PSP's lifetime ratio between the start and end of tests. For both the block and no-block cases, the lifetime ratio decreased with increased exposure time. These data showed that photodegradation progressively reduced the fast-PSP's lifetime ratio. The varying lifetime ratio led to inconsistencies in measurement interpretation. These observations, seen in Fig. 1(b,c) and Fig. 2(a-c), of varying normalized intensity and lifetime ratio across the surface of the model, motivated us to further investigate photodegradation in ISSI porous, fast-response PSP under varying pressures.

3. Benchtop Experiments

Benchtop experiments were conducted in a controlled environment to investigate photodegradation effects on fast-PSP. The benchtop setup allowed for the quantification of changes in luminescent intensity, lifetime ratios, and calibration parameters, highlighting how these factors were influenced by photodegradation under different pressures.

3.1 *Test Chamber Experimental Setup and Data Processing*

To perform all benchtop experiments, an ISSI CAL-04 PSP/TSP calibration system was used. This system consisted of a test chamber where temperature and P_{O2} were controlled with cooling water and O_2/N_2 flows, respectively. The desired temperature and P_{O2} were set on a control box, which adjusted gas and water flow rates to reach the desired condition. Fig. 3(a) shows the chamber in the experimental configuration used. A Phantom v2512 high-speed camera was used for data acquisition, and an ISSI LM4X-DM-400 LED lamp was used for illumination, both operating at 10 kHz. Lamp and camera timing were controlled with an external pulse generator. A close-up image of the test chamber was shown in Fig. 3(b); a paint sample was secured to the copper interface with thermal compound using a copper retaining

clip and a plastic retaining ring mount. Also visible were the gas and water lines to the test chamber.

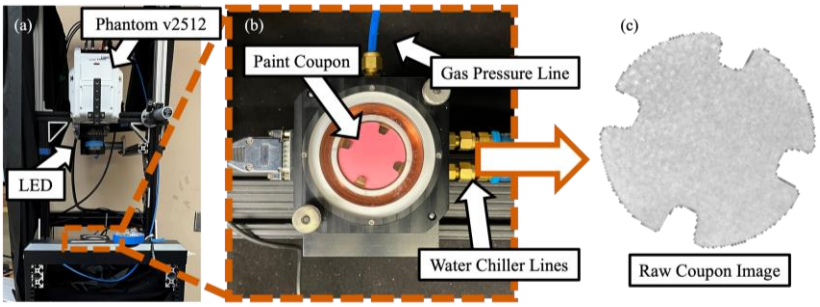

Fig. 3. (a) Paint calibration setup showing the camera, light source, water chiller, and placement of the test chamber; (b) pressure and temperature-controlled test chamber with the painted coupon inside; (c) camera view of the paint coupon with the data mask applied.

A representative raw image of a paint coupon used for testing is shown in Fig. 3(c). The paint coupons were thin aluminum disks 50.8 mm in diameter and were prepared by first applying the ISSI base coat using a high-volume, low-pressure spray gun. This base coat, a 95:5 mixture of Part A and Part B from ISSI, combines Part A, a milky white solution composed mostly of water, with Part B, a solution primarily containing acrylic polymer, to form a porous matrix that dries white, providing a uniform, opaque background [53]. The ISSI topcoat, Part C, consists of a 99% benzotrifluoride solution with PtTFPP dissolved as the pressure-sensitive luminophore and was applied similarly 30 minutes before the testing. The coupons were then stored in a dark area to minimize light exposure until testing began. A series of experiments were conducted to investigate the photodegradation behavior of fast-PSP under varying pressures using four coupons. The experiments had three phases: initial calibration, photodegradation, and final calibration.

For the calibrations, the sensitivity of the fast-PSP to temperature and pressure was determined for each paint coupon. The calibration process involved exposing each coupon to a matrix of three temperatures (15°C, 20°C, and 25°C) and seven partial pressures of oxygen (0, 4.2, 8.4, 12.6, 16.8, 21, and 25.2 kPa). The temperatures were selected because they are near room temperature and representative of the typical range of NASA wind tunnel conditions. Temperature was monitored using a thermocouple positioned below the coupon in the test chamber. The P_{O2} in each case was controlled by adjusting the mole fraction of oxygen flowing into the chamber while maintaining constant absolute pressure and continuous flow. The chamber was purged with 99.999% ultra-high-purity (UHP) N_2 from Airgas (pure UHP N_2 was defined as our 0 kPa P_{O2} condition) or mixtures of UHP N_2 and 99.994% UHP O_2 (to achieve other P_{O2} values) for 20 seconds before recording began, continuing until recording ended. The timing of the lamp illumination and camera gating during calibration is illustrated in Fig. 4(a). For each condition, the lamp was turned on and the camera recorded for one second, collecting 10,000 images to construct the calibration.

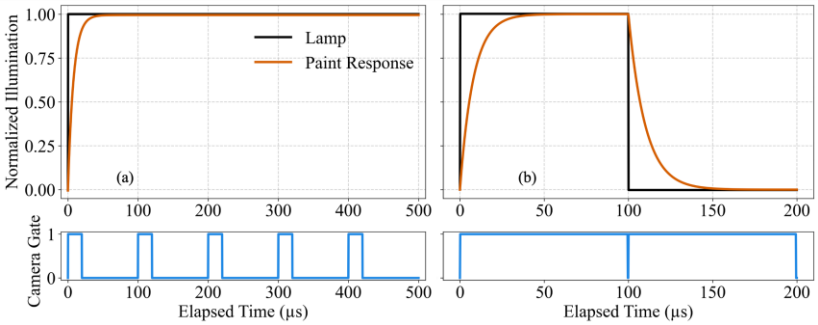

Fig. 4. Lamp illumination, camera gating, and resulting paint response with a representative 10 μs time constant for (a) calibration data acquisition timing (b) lifetime and intensity data acquisition timing.

After the initial calibration, the photodegradation phase was conducted to study how pressure affects the rate of photodegradation. Each coupon was exposed to a different oxygen partial pressure (0, 12.6, 21, or 27.3 kPa) for 14.9 minutes at 20°C. The photodegradation time was limited by the onboard camera memory. During photodegradation, the fast-PSP intensity response was measured continuously at 10 kHz. The lamp operated at a 50% duty cycle, and its illumination and camera gating were controlled by a BNC 575 Digital Delay/Pulse Generator, as illustrated in Fig. 4(b). Each cycle produced two images: the first, captured with the lamp on for 99.965 μs, recorded the initial luminescent response, while the second, captured with the lamp off for 99.965 μs, recorded the decay. Using this method, data for both intensity and lifetime ratio analysis were collected simultaneously. Once the photodegradation phase was completed, a final, post-photodegradation calibration was performed in the same way as the initial to assess changes in the fast-PSP's calibration.

After data collection, the images were analyzed. The intensity method used only the lamp-on images from the photodegradation phase, whereas the lifetime method calculated the ratio from both images as given by Eq. (1):

$$L = \frac{I_{off}}{I_{on}} \tag{1}$$

where I_{off} and I_{on} were the intensities with the lamp off and on, respectively. Data masks were applied in post-processing to isolate the paint pixels. Mean intensities were averaged over 3,000 frames, and a unique mask was used for each coupon to minimize shot noise from the camera, which was applied consistently throughout the analysis. The first-order Stern-Volmer equation was used to consider oxygen quenching effects on intensity [13, 47, 58]:

$$\frac{I_0}{I} = 1 + k_q[O_2] \tag{2}$$

where I_0 was the intensity of the fast-PSP without oxygen quenching (at 0 kPa), I was the intensity of the paint, k_q was the quenching constant, and $[O_2]$ was the concentration of oxygen. According to Henry's Law, the concentration of oxygen that permeates into the paint is directly proportional to the partial pressure [46, 59, 60]. Therefore, the oxygen can be expressed as P/P_{ref}, where P_{ref} is the reference pressure used to avoid division by zero [46]. The reference pressure corresponds to the wind-off condition in the wind tunnel, equivalent to 100 kPa of air or 21 kPa of oxygen. In practice, a nonlinear term was often included to account for nonconformities and highlight deviations from ideal behavior [61, 62]. The modified Stern-Volmer equation used for curve fitting was [46, 50]:

$$\frac{I_0}{I} = A + B\left(\frac{P}{P_{ref}}\right) + C\left(\frac{P}{P_{ref}}\right)^2 \quad (3)$$

where A, B, and C were calibration fit constants, and P was the pressure. By comparing the calibration curves before and after photodegradation, the accuracy across extended exposure times could be evaluated.

An uncertainty analysis was conducted to determine the statistical significance of the observed trends in the benchtop experiments. By analyzing the central area of the coupons and calculating the uncertainty defined by 2σ of the pixel intensities, the uncertainty was determined to be 3.5% of the mean. The absolute uncertainty in the initial intensity (3300 counts) of the coupon shown in Fig. 3 is ± 116 counts. This baseline uncertainty accounts for factors such as paint coat unevenness, camera noise, variation in excitation light intensity, angle of incidence, and fluctuations in environmental conditions.

3.2 *Luminescent Intensity Measurements*

The effect of photodegradation on the luminescent intensity and its impact under various partial pressures was evaluated first. Intensity data were continuously recorded during the 14.9-minute experiments for each of the four paint coupons. The normalized intensities over time for each coupon are presented in Fig. 5(a). The intensity of the fast-PSP decreases steadily with prolonged exposure to excitation light, with the rate of decline varying based on the partial pressure of oxygen during exposure to excitation light. At a photodegradation pressure of 0 kPa, the signal decreases the least since the absence of oxygen prevents photo-oxidation, and the signal decreases to 71% of its initial intensity at the end of the experiment due solely to photodecomposition. In contrast, for cases with oxygen exposure, both photodecomposition and photo-oxidation contribute to photodegradation, which led to a more significant signal decrease [29, 41, 42]. At 27.3 kPa, the intensity decreases to 31% of the initial intensity at the end of the experiment, less than half of that observed at 0 kPa. This trend is consistent with observations from the wind tunnel tests, where regions exposed to higher pressures had greater intensity decreases, as shown in Fig. 1.

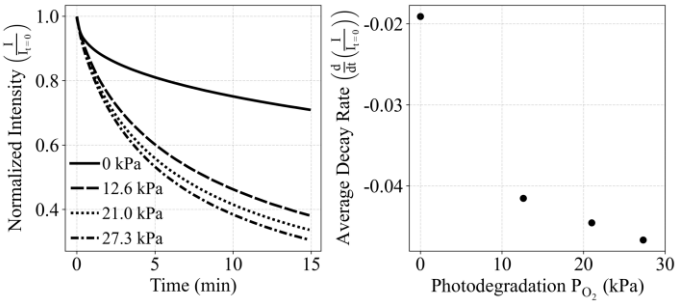

Fig. 5. (a) Paint coupon intensity of lamp-on frames during photodegradation under various pressures. (b) Average intensity rate of decrease over the 14.9-minute experiment as a function of photodegradation pressure.

By evaluating the average rate of decay in the normalized intensity, as shown in Fig. 5(b), it is observed that the photodegradation rate is greater with increasing P_{O2} during photodegradation. When the photodegradation pressure is 0 kPa, where photodegradation occurs solely through photodecomposition, the average decay rate is 1.9% per minute. At a photodegradation pressure of 27.3 kPa, where both photodecomposition and photo-oxidation contribute, the average decay rate is 4.7% per minute. These measured photodegradation rates

differ from ISSI's reported photodegradation rate of 1% per minute; ISSI's reported value does not account for lamp intensity, oxygen partial pressure during photodegradation, or the nonlinearity of photodegradation over time [53]. A linear fit to the data in Fig. 5(b) reveals that the intensity decay rate increases by 0.10% per minute per kPa of P_{O2}. This indicates that the additional intensity decrease is driven by photo-oxidation. These observations confirm that oxygen accelerates photodegradation, and this metric quantifies the extent.

3.3 *The Lifetime Method*

The effect of photodegradation on the lifetime method under varying pressures is also evaluated through the benchtop experiments. The experiments tracked changes in lifetime ratios, as described in Eq. 1, for the four paint coupons exposed to different pressures over the 14.9-minute period. Fig. 6(a) shows the normalized lifetime ratio of each coupon during photodegradation at various partial pressures of oxygen. The normalized lifetime ratios decline more rapidly at higher pressures, similar to the trend observed in the fast-PSP intensity shown in Fig. 5(a). At the end of the experiment, the highest photodegradation pressure case shows the final lifetime ratio is 26% of the initial. The 0 kPa case shows a decrease to 77% of the initial lifetime ratio. Although photo-oxidation does not contribute at 0 kPa, photodecomposition did. Fig. 6(b) further quantifies this trend and shows the average decay rate of the lifetime ratio, with a measured average rate of 1.5% per minute at 0 kPa and 5% per minute at 27.3 kPa. A linear fit to the data reveals that the lifetime ratio average rate of decay increases by 0.12% per minute per kPa of P_{O2}. These observations confirm that oxygen accelerates photodegradation, which leads to faster declines in the lifetime ratio. Moreover, the decline in the lifetime ratio is more substantial at higher photodegradation pressures, similar to trends observed in the intensity measurements. Of interest is the apparent relationship between pressure during photodegradation and rate of lifetime ratio decrease, which the authors have not seen previously reported in the literature.

The decreasing lifetime ratio as the fast-PSP photodegrades suggests that the decay time constant of the luminophore decreases with excitation light exposure, which signals that photodecomposition and photo-oxidation might alter the structure of the luminescent dye. Although the lifetime method reduces some of the errors caused by photodegradation, corrections remain necessary for accurate pressure measurements.

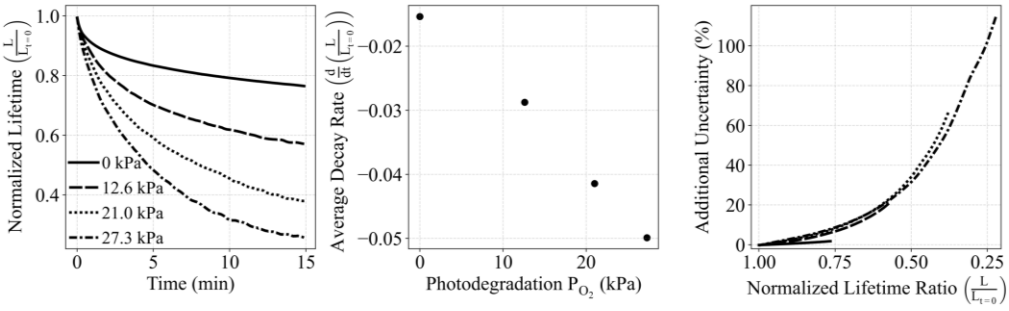

Fig. 6. (a) Normalized lifetime ratio of each coupon during photodegradation. (b) Average lifetime ratio rate of decrease over the 14.9-minute experiment as a function of photodegradation partial pressure. (c) Additional uncertainty in the normalized lifetime ratio as a percent of the mean during fast-PSP photodegradation.

Photodegradation leads to an increase in measurement uncertainty relative to the initial uncertainty measured at the beginning of the photodegradation phase. This additional uncertainty is expressed as a percentage increase over the baseline uncertainty and is plotted in Fig. 6(c) versus the normalized lifetime ratio. As the lifetime ratio decreases due to exposure to an excitation source, the uncertainty increases nonlinearly for all photodegradation pressures.

Since the coupon photodegraded at 27.3 kPa experiences the greatest decline in its lifetime ratio, it shows the highest accumulated uncertainty after 14.9 minutes. These findings are particularly relevant for wind tunnel testing, where different pressure regions photodegrade at varying rates. This causes both the lifetime ratio and measurement uncertainty to become inconsistent across the model and complicates accurate pressure measurements. Table 1 summarizes the uncertainty increases observed during photodegradation for lifetime ratio decreases of 5%, 10%, and 20%, which demonstrate that higher photodegradation pressures led to greater accumulated uncertainty.

Table 1. Additional uncertainty in fast-PSP lifetime ratio due to photodegradation at different pressures

Photodegradation Pressure (kPa)	Additional uncertainty at 0.95 normalized lifetime ratio (%)	Additional uncertainty at 0.9 normalized lifetime ratio (%)	Additional uncertainty at 0.8 normalized lifetime ratio (%)	Additional uncertainty after 14.9 minutes (%)
0	0.17	0.52	1.37	1.76
12.6	0.64	1.64	4.64	20.80
21	1.03	2.25	5.65	66.62
27.3	1.33	2.62	6.25	114.73

3.4 *Calibration Accuracy*

To evaluate how photodegradation affects the calibration, the post-photodegradation final calibration is compared to the initial calibration. As discussed previously, both calibrations were performed identically, which ensured any differences observed were solely due to photodegradation. This comparison was used to determine changes in pressure sensitivity and overall calibration accuracy.

Fig. 7(a,b) shows the calibration curve fits before and after photodegradation for the coupons with the lowest and highest photodegradation pressures, respectively. The nondimensionalized intensity is plotted versus nondimensionalized pressure. Here, the different calibration temperatures are indicated with different colors, and the initial calibration is shown with solid lines and the final with dashed lines. The initial calibration curves across coupons were similar, which was expected given the coupons were not photodegraded. After 14.9 minutes of photodegradation, both coupons showed lower intensity for a given pressure and increased nonlinearity in the calibration curves. The decrease in pressure sensitivity and degree of nonlinearity is more pronounced for the coupon photodegraded at 27.3 kPa. This change in the calibration curves is due to an increased nonlinear component, as described in Eq. 3. Overall, these results showed that photodegradation, especially at higher P_{O2}, compromises the accuracy of calibration curves.

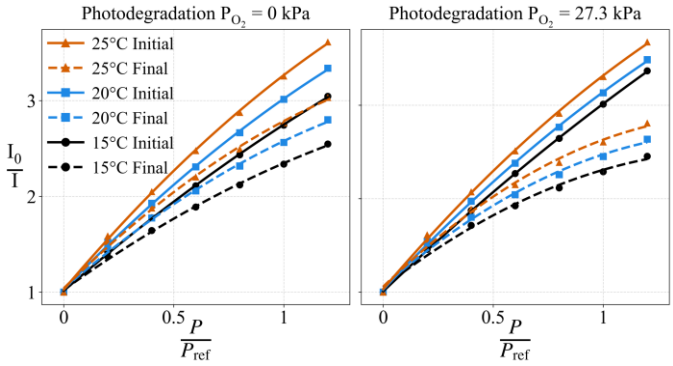

Fig. 7. Calibration curve fits for two of the photodegraded coupons at varying photodegradation pressures, (a) 0 kPa and (b) 27.3 kPa, which shows isothermal calibration curves at three different temperatures.

To evaluate the impact of photodegradation on calibration accuracy, pressure measurements are compared using the initial and final calibration curves. A single curve is generated for the final calibration with all three temperature values for each pressure averaged together. Plotted in Fig. 8(a) is the pressure that would be reported if the initial calibration is used after photodegradation. The difference between the actual and reported values quantifies the error introduced by photodegradation. The data shows that after 14.9 minutes of photodegradation, the reported pressure becomes increasingly overestimated relative to the actual pressure. This overestimation is greater with higher photodegradation pressures. The coupon photodegraded at 0 kPa, photodegrading primarily via photodecomposition, shows a noticeable error. However, this error is lower than that observed for the coupon photodegraded at 27.3 kPa, where photodegradation results from both photodecomposition and photo-oxidation.

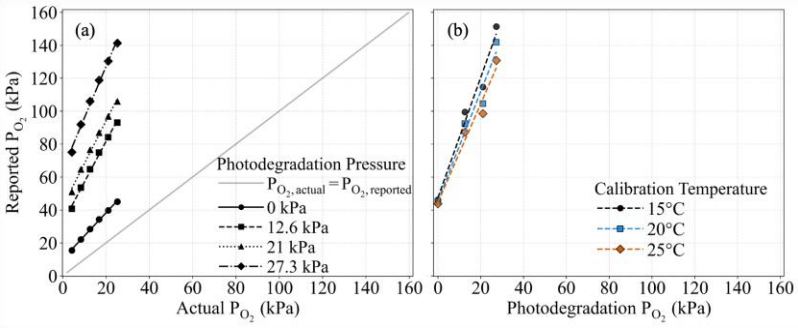

Fig. 8 (a) The reported pressure measurement after 14.9 minutes of photodegradation if the initial calibration was used. (b) Measured pressure versus actual pressure for different isothermal calibration curves using data from the 25.2 kPa actual pressure.

Two key trends emerge from these results. First, as photodegradation pressure increases, the calibration curves shift upward, which means that all reported pressures are overestimated relative to the actual values. This highlights that the intensity drop caused by photodegradation mimics the effect of higher pressures and leads to significant errors if the initial calibration is used. Second, the slope of the calibration curves steepens with increasing photodegradation pressure, which means that the calibration data points recorded at higher pressures are more affected by photodegradation. This suggests that photodegradation not only causes an overestimation of pressure but does so in a complex manner, which makes it more difficult to determine accurate pressure values from sufficiently photodegraded fast-PSP.

Fig. 8(b) shows the relationship between photodegradation pressure and the reported pressure for the three calibration temperatures. This plot is generated with the data from an actual oxygen partial pressure of 25.2 kPa, which corresponds to the rightmost points in Fig. 8(a). Rather than all final calibration data points displayed, Fig. 8(b) plotted the reported pressure at one calibration pressure as a function of photodegradation pressure. Linear fits show that as photodegradation pressure increases, the reported pressure is increasingly overestimated. The 15°C fit has the highest reported pressures and the steepest slope, while the 25°C case has the lowest reported pressures and the least steep slope. The differences in the 15°C and 25°C cases show that the calibration data points recorded at lower temperatures are more affected by photodegradation, further demonstrating that the resulting calibration changes are complex.

Photodegradation affects the intensity-pressure relationship, particularly when photodegraded at higher pressures, and recalibration is necessary to maintain accurate measurements. As the paint photodegraded, the intensity of the paint decreased, mimicking higher pressures. When the intensity values after significant photodegradation are used with the initial calibration curve taken at the beginning of a wind tunnel run, the calculated pressures are significantly overestimated.

For the intensity method, lifetime method, and calibration, the fast-PSP photodegradation is accelerated at higher pressures and longer exposure times. Photodegradation reduces intensity and lifetime ratios and introduces nonlinearity into calibration curves. Significant errors in pressure measurements can occur if not properly accounted for.

4. Recommendations and Best Practices

Photodegradation introduced additional uncertainty to fast-PSP measurements, especially in regions with steep pressure gradients, as illustrated in Fig. 6(c). The nonlinear decrease in intensity with exposure to an excitation source compounds this effect; higher-pressure regions experience more rapid photodegradation and higher measurement errors compared to lower-pressure regions. Despite the challenges posed by photodegradation, effective strategies can be implemented to use PtTFPP-based porous, fast-response PSP and still deliver accurate, reliable results. These best practices should also be considered for other oxygen-sensor PSP formulations, especially those that use PtTFPP, as they likely have similar photodegradation characteristics due to shared mechanisms. To mitigate the effects of photodegradation and ensure reliable fast-PSP measurements, the following practices are recommended:

- Pair fast-PSP measurements with "truth" measurements, such as a pressure transducer, to continuously calibrate the PSP and minimize uncertainty.
- Minimize light exposure time between fast-PSP measurements.
- Monitor fast-PSP-coated surfaces during testing for spatially inconsistent decreases in intensity. Replace the paint coating if the intensity falls significantly below its initial level or shows inconsistent photodegradation across the surface.
- Reapply fast-PSP coatings when necessary, especially for experiments with large models or regions with steep pressure gradients, where photodegradation-induced uncertainty accumulates more quickly.
- Recalibrate to account for photodegradation effects when reapplication is not feasible, or photodegradation is unavoidable.
- Define acceptable uncertainty thresholds based on the specific application and experimental requirements to guide decisions on reapplication and calibration frequency.

The uncertainties in the lifetime ratio will appear in processed images as nonuniformities, particularly in regions with steep pressure gradients. Such nonuniformities have been previously observed and discussed in [17, 24, 45, 52]. Table 1 and Fig. 6(c) quantify the uncertainties introduced by photodegradation across different photodegradation pressures. Ultimately, the acceptable level of uncertainty and photodegradation limits will depend on the

intended application and experimental constraints, such as error tolerance, pressure gradient, model size, and coating uniformity.

5. Conclusions

The effects of photodegradation in pressure-sensitive paint were studied in benchtop experiments using ISSI porous, fast-response PSP. Changes in luminescent intensity, lifetime ratios, and calibration curves were measured across varying pressures. When exposed to an excitation source, the rate of luminescent intensity decrease was greater at higher pressures, consistent with wind tunnel data. In the benchtop experiments, intensity decreased to 31% of the initial intensity at a photodegradation pressure of 27.3 kPa with an average decay rate of 4.7% per minute, compared to only 71% at 0 kPa with an average decay rate of 1.9% per minute after 14.9 minutes of exposure. Similarly, the lifetime ratio of the paint decreased with exposure to an excitation source, indicating a change in the time constant as the fast-PSP photodegrades. The lifetime ratio decreased to 26% of the initial at a photodegradation 27.3 kPa with an average decay rate of 5% per minute, versus 77% at 0 kPa with an average decay rate of 1.5% per minute over the same period. These average decay rates varied with photodegradation pressure, as the experiments further revealed that the luminescent intensity decay rate increased by 0.10% per minute per kPa of P_{O2}, and the lifetime ratio decay rate increased by 0.12% per minute per P_{O2}. These findings show that the rate of decrease in both the intensity and the lifetime ratio during photodegradation is pressure dependent.

In the benchtop tests, initial fast-PSP calibration curves exhibited a nearly linear relationship between normalized intensity and normalized pressure. However, after photodegradation, recalibration showed a pronounced overestimation of pressure and increased nonlinearity in the calibration curves, resulting in reduced pressure sensitivity. Using the initial calibration curve to interpret the photodegraded intensity values resulted in a significant overestimation of pressure readings. If photodegradation was neglected, significant overestimations of pressure occurred, particularly at higher photodegradation pressures and longer exposure times. The overestimation varies widely after the 14.9 minutes, where at a photodegradation pressure of 0 kPa, the shift is 11.3 kPa, whereas at 27.3 kPa, this shift is 115.5 kPa.

Our findings suggested that the characteristics of fast-PSP photodegradation were consistent with both photodecomposition and photo-oxidation processes taking place on the luminophore of the paint when exposed to oxygen and excitation light. Photodegradation occurs in the paint, even in the absence of oxygen due to photodecomposition, but the presence of oxygen accelerates photodegradation through photo-oxidation.

To mitigate these effects, fast-PSP should be reapplied based on the specific experimental requirements and be paired with “truth” measurements throughout the model while minimizing light exposure time between measurements to limit photodegradation. For tests with steep pressure gradients, where photodegradation occurs unevenly, more frequent calibrations and reapplication of fast-PSP may be necessary to maintain accurate and reliable pressure measurements. When reapplication is impractical or if photodegradation is unavoidable, recalibration should account for photodegradation effects. By understanding the results of photodegradation on fast-PSP, it can be better maintained to ensure accurate pressure measurements, even under varying pressures and exposure conditions.

Funding. NASA (80NSSC19M0194)

Acknowledgment. The authors would like to thank the rest of the uPSP test team at the NASA Ames Research Center, including Marc Shaw-Lecerf and Nicholas Califano, for their invaluable assistance in acquiring, processing, and discussing the fast-PSP data analyzed in this paper. The authors would also like to thank the NASA MUREP Institutional Research Opportunity (MIRO) for sponsoring this internship under the MIRO 7 UTSA funding source administered by Guardians of Honor, LLC (GOH). The project also received funding from the NASA Aeronautics Research Mission Directorate's (ARMD) and Aerosciences Evaluation and Test Capabilities (AETC) Portfolio Office.

Disclosures. The authors declare no conflicts of interest.

Data availability. Data underlying the results presented in this paper are not publicly available at this time but may be obtained from the authors upon reasonable request.

References

1. N. Roozeboom, J. Powell, J. Baerny et al., "Development of unsteady pressure-sensitive paint application on NASA space launch system," in *AIAA Aviation 2019 Forum*(2019), p. 3502.
2. N. Roozeboom, S. M. Murman, L. Diosady et al., "Unsteady PSP measurements on a rectangular cube," in *54th AIAA Aerospace Sciences Meeting*(2016), p. 2017.
3. J. Panda, "Experimental verification of buffet calculation procedure using unsteady pressure-sensitive paint," Journal of Aircraft **54**, 1791-1801 (2017).
4. J. M. Powell, S. M. Murman, C. Ngo et al., "Development of unsteady-PSP data processing and analysis tools for the NASA AMES UNITary 11ft wind tunnel," in *AIAA Scitech 2020 Forum*(2020), p. 0292.
5. E. L. Lash, N. Roozeboom, J. K. Baerny et al., "Preliminary Unsteady Characterization of Shock Wave/Boundary Layer Interactions on a 4% Scale SLS Model using uPSP and Shadowgraph," in *AIAA AVIATION 2020 FORUM*(2020), p. 2725.
6. J. Li, E. L. Lash, N. Roozeboom et al., "Dynamic Mode Decomposition of Unsteady Pressure-Sensitive Paint Measurements for the NASA Unitary Plan Wind Tunnel Tests," in *AIAA SCITECH 2022 Forum*(2022), p. 0141.
7. D. M. Schuster, J. Panda, J. C. Ross et al., "Investigation of unsteady pressure-sensitive paint (uPSP) and a dynamic loads balance to predict launch vehicle buffet environments," (2016).
8. M. E. Sellers, M. A. Nelson, N. J. Burnside et al., "Evaluation of Unsteady Pressure Sensitive Paint Use for Space Launch Vehicle Buffet Determination," in *55th AIAA Aerospace Sciences Meeting*(2017), p. 1402.
9. A. Andrade, E. J. LaLonde, E. N. Hoffman et al., "Application of Pressure-Sensitive Paint to Investigate Hypersonic Shock-Wave/Boundary-Layer Interactions," in *AIAA SCITECH 2023 Forum*(2023), p. 1178.
10. Y. Sugioka, H. Sato, K. Nakakita et al., "In-Flight visualization of shock wave on a jet aircraft wing using lifetime-based pressure-sensitive paint technique," in *AIAA Scitech 2019 Forum*(2019), p. 0024.
11. N. Roozeboom, C. Ngo, J. M. Powell et al., "Data Processing Methods for Unsteady Pressure-Sensitive Paint Application," in *2018 AIAA Aerospace Sciences Meeting*(2018), p. 1031.
12. V. Delgado Elizondo, A. Dhanagopal, and C. S. Combs, "Fast-Responding Pressure-Sensitive Paint Measurements of the IC3X at Mach 7.2," Aerospace **10**, 890 (2023).
13. J. Kavandi, J. Callis, M. Gouterman et al., "Luminescent barometry in wind tunnels," Review of Scientific Instruments **61**, 3340-3347 (1990).
14. K. Asai, K. Nakakita, M. Kameda et al., "Recent topics in fast-responding pressure-sensitive paint technology at National Aerospace Laboratory," in *ICIASF 2001 Record, 19th International Congress on Instrumentation in Aerospace Simulation Facilities (Cat. No. 01CH37215)*(IEEE2001), pp. 25-36.
15. K. Asai, Y. Amao, Y. Iijima et al., "Novel pressure-sensitive paint for cryogenic and unsteady wind-tunnel testing," Journal of thermophysics and heat transfer **16**, 109-115 (2002).
16. D. Yorita, U. Henne, and C. Klein, "Improvement of lifetime-based PSP technique for industrial wind tunnel tests," in *55th AIAA Aerospace Sciences Meeting*(2017), p. 0703.
17. W. Ruyten, M. Sellers, and W. Baker, "Spatially nonuniform self-quenching of the pressure-sensitive paint PtTFPP/FIB," in *47th AIAA Aerospace Sciences Meeting including The New Horizons Forum and Aerospace Exposition*(2009), p. 1660.

18. J. W. Gregory, H. Sakaue, T. Liu et al., "Fast pressure-sensitive paint for flow and acoustic diagnostics," Annual Review of Fluid Mechanics **46**, 303-330 (2014).
19. J. Bell, "Pressure-sensitive paint measurements on the NASA common research model in the NASA 11-ft transonic wind tunnel," in *49th AIAA Aerospace Sciences Meeting including the New Horizons Forum and Aerospace Exposition*(2011), p. 1128.
20. J. H. Bell, E. T. Schairer, L. A. Hand et al., "Surface pressure measurements using luminescent coatings," Annual Review of Fluid Mechanics **33**, 155-206 (2001).
21. R. Crites, and M. Benne, "Emerging technology for pressure measurement-pressure sensitive paint," in *33rd Aerospace Sciences Meeting and Exhibit*(1995), p. 106.
22. J. W. Gregory, K. Asai, M. Kameda et al., "A review of pressure-sensitive paint for high-speed and unsteady aerodynamics," Proceedings of the institution of mechanical engineers, part G: journal of aerospace engineering **222**, 249-290 (2008).
23. Y. Sugioka, K. Nakakita, K. Saitoh et al., "First results of lifetime-based unsteady PSP measurement on a pitching airfoil in transonic flow," in *2018 AIAA aerospace sciences meeting*(2018), p. 1030.
24. D. D. Murakami, M. Shaw-Lecerf, E. L. Lash et al., "Implementation of the Lifetime Method in Unsteady Pressure-Sensitive Paint Measurements," in *AIAA SCITECH 2023 Forum*(2023), p. 0635.
25. N. Roozeboom, and J. K. Baerny, "Customer Guide to Pressure-Sensitive Paint Testing at NASA Ames Unitary Plan Wind Tunnels," in *55th AIAA Aerospace Sciences Meeting*(2017), p. 1055.
26. M. K. Quinn, L. Yang, and K. Kontis, "Pressure-sensitive paint: effect of substrate," Sensors **11**, 11649-11663 (2011).
27. S. Nagl, and O. S. Wolfbeis, "Optical multiple chemical sensing: status and current challenges," Analyst **132**, 507-511 (2007).
28. C.-S. Chu, and C.-A. Lin, "Optical fiber sensor for dual sensing of temperature and oxygen based on PtTFPP/CF embedded in sol–gel matrix," Sensors and Actuators B: Chemical **195**, 259-265 (2014).
29. Y. Egami, and K. Asai, "Effects of antioxidants on photodegradation of porous pressure-sensitive paint," in *22nd AIAA Aerodynamic Measurement Technology and Ground Testing Conference*(2002), p. 2905.
30. L. Goss, D. Trump, B. Sarka et al., "Multi-dimensional time-resolved pressure-sensitive-paint techniques-a numerical and experimental comparison," in *38th Aerospace Sciences Meeting and Exhibit*(2000), p. 832.
31. W.-C. Chen, C.-Y. Huang, K.-T. Tan et al., "The development and application of two-color pressure-sensitive paint in jet impingement experiments," Aerospace **10**, 805 (2023).
32. K. Uchida, K. Nakakita, Y. Sugioka et al., "Dual-luminophore pressure-sensitive paint measurement using three-gate lifetime method with photodegradation correction," Review of Scientific Instruments **95** (2024).
33. A. T. Rendon, V. V. Granado, and C. S. Combs, "Application and Calibration of Steady Pressure Sensitive Paint at a Hypersonic Ludwieg Tube Wind Tunnel."
34. K. Uchida, K. Nakakita, and T. Nonomura, "Dual-Luminophore Pressure-Sensitive Paint Measurement of Vertical Tail Model Using Three-Gate Liftime Method With Photodegradation Correction," in *AIAA SCITECH 2025 Forum*(2025), p. 1065.
35. K. Uchida, Y. Ozawa, K. Asai et al., "Reducing Photodegradation of Dual-Luminophore Pressure-Sensitive Paint by Adding Antioxidants," in *AIAA SCITECH 2023 Forum*(2023), p. 0227.
36. K. H. Lo, and K. Kontis, "Static and wind-on performance of polymer-based pressure-sensitive paints using platinum and ruthenium as the luminophore," Sensors **16**, 595 (2016).
37. M. Kasai, D. Sasaki, T. Nagata et al., "Frequency response of pressure-sensitive paints under low-pressure conditions," Sensors **21**, 3187 (2021).

38. Y. Egami, Y. Sato, and S. Konishi, "Development of sprayable pressure-sensitive paint with a response time of less than 10 μ s," AIAA journal **57**, 2198-2203 (2019).
39. M. Kasai, T. Nagata, K. Uchida et al., "Evaluation of characteristics of fast-response pressure-sensitive paint under low-pressure conditions," Measurement Science and Technology **34**, 075103 (2023).
40. B. J. Basu, C. Anandan, and K. Rajam, "Study of the mechanism of degradation of pyrene-based pressure sensitive paints," Sensors and Actuators B: Chemical **94**, 257-266 (2003).
41. E. Yousif, and R. Haddad, "Photodegradation and photostabilization of polymers, especially polystyrene," SpringerPlus **2**, 1-32 (2013).
42. K. Uchida, Y. Ozawa, K. Asai et al., "Photostability enhancement of dual-luminophore pressure-sensitive paint by adding antioxidants," Sensors **22**, 9470 (2022).
43. J. H. Bell, "Accuracy limitations of lifetime-based pressure-sensitive paint (PSP) measurements," in *ICIASF 2001 Record, 19th International Congress on Instrumentation in Aerospace Simulation Facilities (Cat. No. 01CH37215)*(IEEE2001), pp. 5-16.
44. A. Davies, D. Bedwell, M. Dunleavy et al., "Pressure sensitive paint measurements using a phosphorescence lifetime method," in *Proceedings of the 7th International Symposium on Flow Visualization*(1995), pp. 11-14.
45. D. Yorita, C. Klein, U. Henne et al., "Improvement of PtTFPP-based PSP for lifetime-based measurement and application to transonic wind tunnel test," (2014).
46. T. Liu, J. P. Sullivan, K. Asai et al., *Pressure and temperature sensitive paints* (Springer, 2005).
47. M. Sellers, "Advances in AEDC's Lifetime Pressure-Sensitive Paint Program," in *2005 US Air Force T&E Days*(2005), p. 7638.
48. W. Ruyten, "Assimilation of physical chemistry models for lifetime analysis of pressure-sensitive paint," AIAA journal **43**, 465-471 (2005).
49. M. Kasai, T. Nagata, T. Nonomura et al., "Optimal gate selection method for simultaneous lifetime-based measurement of PSP and TSP," Measurement Science and Technology **33**, 095203 (2022).
50. S. Torgerson, T. Liu, and J. Sullivan, "Use of pressure sensitive paints in low speed flows," in *Advanced Measurement and Ground Testing Conference*(1996), p. 2184.
51. W. Ruyten, and M. Sellers, "Lifetime analysis of the pressure-sensitive paint PtTFPP in FIB," in *42nd AIAA Aerospace Sciences Meeting and Exhibit*(2004), p. 881.
52. Y. Egami, Y. Yamazaki, N. Hori et al., "Investigation of factors causing nonuniformity in luminescence lifetime of fast-responding pressure-sensitive paints," Sensors **21**, 6076 (2021).
53. S. Paluccioni, "Porous Fast Response Pressure Sensitive Paint Datasheet," https://innssi.com/wp-content/uploads/Pressure_Sensitive_Paint/Porous_Fast_PSP/Documentation/Porous-Fast-Response-PSP-FP-XXX-Data-Sheet.pdf.
54. M. Shaw-Lecerf, E. L. Lash, D. D. Murakami et al., "Methodology for Validation of Unsteady Pressure-Sensitive Paint Measurements using Pressure Transducers," in *AIAA SCITECH 2023 Forum*(2023), p. 0639.
55. D. D. Murakami, L. Hand, K. Lyons et al., "Error Estimation for Unsteady Pressure Sensitive Paint Measurements," in *AIAA SciTech 2025 Forum*(2025), p. 0236.
56. J. W. Crafton, S. Stanfield, N. Rogoshchenkov et al., "Investigation of passive flow control of cavity acoustics using dynamic pressure-sensitive paint," in *55th AIAA aerospace sciences meeting*(2017), p. 1178.
57. N. S. Strasser, D. D. Murakami, E. L. Lash et al., "Characterization of Photodegradation in Unsteady Pressure-Sensitive Paint Under Varying Pressures," in *AIAA AVIATION FORUM AND ASCEND 2024*(2024), p. 4379.

58. O. Stern, and M. Volmer, "Über die abklingungszeit der fluoreszenz," Physikalische Zeitschrift **20**, 183-188 (1919).
59. J. W. Gregory, and J. P. Sullivan, "Effect of quenching kinetics on unsteady response of pressure-sensitive paint," AIAA journal **44**, 634-645 (2006).
60. A. Vollan, and L. Alati, "A new optical pressure measurement system (OPMS)," in *ICIASF'91 Record., International Congress on Instrumentation in Aerospace Simulation Facilities*(IEEE1991), pp. 10-16.
61. P. A. N. Aye-Addo, G. Paniagua, D. G. Cuadrado et al., "Development of a lifetime pressure sensitive paint procedure for high-pressure vane testing," Journal of Turbomachinery **144**, 051005 (2022).
62. A. Dhanagopal, C. Williamson, E. J. LaLonde et al., "High-Speed Pressure Sensitive Paint Measurements of the Initial Concept 3. X Vehicle at Mach 7," in *AIAA SCITECH 2023 Forum*(2023), p. 1179.